J Solid State Eletrochem (2004) 8: 260–271
DOI 10.1007/s10008-003-0445-1

ORIGINAL PAPER

João Pedro Ferreira · João Alexandre Rodrigues
Inês Teodora Elias da Fonseca

Copper corrosion in buffered and non-buffered synthetic seawater: a comparative study

Received: 20 May 2003 / Accepted: 19 August 2003 / Published online: 23 December 2003

Abstract The electrochemical behaviour of copper in neutral buffered and non-buffered synthetic seawater and in pure chloride solutions has been studied by cyclic voltammetry, weight loss measurements, open circuit potential and scanning electron microscopy (SEM). Values of the repassivation potentials of Cu in non-buffered and buffered synthetic seawater, at 50 mV s^{-1}, were 0.12 and 0.46 V vs. SCE, respectively. The sharpness, heights and location of the different peaks as well as their charges were shown to be influenced by the composition of the solution, buffering conditions, deoxygenation, polarization potential and time. High chloride concentrations lead to higher oxidation charges. The anodic and the cathodic charges were shown to increase as the chloride concentration increases. The open circuit potential transients of copper in non-deoxygenated, non-buffered synthetic seawater indicate pitting from the beginning of the exposure, while in buffered solutions the pitting appeared only after a quite long exposure period, i.e. after 40 days. Corrosion rates of Cu samples after 3 months of immersion were higher in solutions of pure chloride (0.5 M) than in synthetic seawater. After six months the differences were even more noticeable. SEM images have showed a somewhat higher density of pits on copper samples immersed in the chloride solution (0.5 M), in comparison with those in synthetic seawater.

Keywords Boric acid/borax buffered seawater · Copper corrosion · Deoxygenation · SEM micrographs · Voltammetric studies

J. P. Ferreira · J. A. Rodrigues · I. T. E. da Fonseca (✉)
Departamento de Química e Bioquímica,
Centro de Electroquímica e Cinética da Universidade de Lisboa,
R. Ernesto Vasconcelos, Ed. C8, 1749-016 Lisbon, Portugal
E-mail: itfonseca@fc.ul.pt
Tel.: +351-21-7500904
Fax: +351-21-7500892

Introduction

The corrosion, passivation and breakdown of passivity of copper have been studied over a wide range of experimental conditions [1, 2, 3, 4, 5, 6, 7, 8, 9, 10, 11, 12, 13, 14, 15, 16, 17, 18, 20, 21, 22, 23, 24, 25, 26, 27, 28, 29, 30, 31, 32, 33, 34, 35, 36, 37, 38, 39, 40, 41, 42, 43, 44, 45, 46, 47, 48, 49, 50].

According to various authors, in the absence of aggressive anions the passivation of copper in alkaline solutions is due to an oxide layer whose electrochemical characteristics and structure depend on the solution composition and the applied polarization potential [1, 2, 3, 4, 5, 6, 7, 8, 9, 10, 11, 12, 13, 14, 15, 16, 17, 18]. In alkaline media, cyclic voltammograms exhibit various peaks that have been assigned to Cu(I), Cu(II) and Cu(III) species and a multiplicity of cathodic peaks related to the reduction of different soluble and insoluble copper-containing species [1, 2, 3, 4, 5, 6, 7, 8, 9, 10, 11, 12, 13, 14, 15, 16, 17, 18].

In the absence of aggressive anions, the structure of the passive Cu layer in borate buffer, as revealed by ESCA and ISS, consists of inner Cu_2O and outer CuO hydrated layers [8]. In the potential region of oxygen evolution, some authors have detected an additional anodic peak. This peak has been attributed to the formation of Cu(III) oxide species (Cu_2O_3) and/or to the formation of soluble complex copper-containing species [1, 2, 3, 7, 31]. According to Pourbaix [19], in the absence of aggressive anions, Cu in neutral aqueous solutions may lead to the formation of solid species, i.e.:

$$2Cu + H_2O \rightarrow Cu_2O + 2H^+ + 2e^- \qquad E_e = +0.471 - 0.0591pH \tag{1}$$

$$Cu + H_2O \rightarrow CuO + 2H^+ + 2e^- \qquad E_e = +0.570 - 0.0591pH \tag{2}$$

$$Cu + 2H_2O \rightarrow Cu(OH)_2 + 2H^+ + 2e^- \qquad E_e = +0.609 - 0.0591pH \tag{3}$$

$$Cu_2O + H_2O \rightarrow 2CuO + 2H^+ + 2e^- \quad E_e = +0.669 - 0.0591pH \tag{4}$$

$$Cu_2O + H_2O + 2OH^- \rightarrow 2Cu(OH)_2 + 2e^- \quad E_e = +0.747 - 0.059pH \tag{5}$$

$$2Cu(OH)_2 \rightarrow Cu_2O_3 + H_2O + 2e^- \quad E_e = +1.578 - 0.059pH \tag{6}$$

$$2CuO + H_2O \rightarrow Cu_2O_3 + 2H^+ + 2e^- \quad E_e = +1.648 - 0.059pH \tag{7}$$

During the anodic polarization of copper in neutral and alkaline solutions, soluble copper species, i.e. Cu^+, Cu^{2+}, Cu^{3+}, $HCuO^{2-}$ and CuO_2^{2-}, can be formed. Their amount and nature depend on the solution pH and the applied polarization potential. Soluble copper-containing species have been identified by RRDE studies [2, 5, 7, 8, 9, 12, 47].

In aqueous solutions in the presence of O_2 (non-deoxygenated solutions), the reduction of O_2 leads to the formation of OH^-, according to the reaction:

$$O_2 + 2H_2O + 4e^- \rightarrow 4OH^- \qquad E_e = +1.229 - 0.059pH \tag{8}$$

while in the absence of O_2, the reduction of H_2O leads also to the formation of OH^- species, but this process occurs at much lower potentials, according to:

$$2H_2O + 2e \rightarrow H_2 + 2OH^- \qquad E_e = 0.00 - 0.059pH \tag{9}$$

The corrosion, passivation and transpassive corrosion of copper in the presence of aggressive anions, i.e. HCO_3^-, Cl^- or SO_4^{2-}, has also been investigated by many researchers [20, 21, 22, 23, 24, 25, 26, 27, 28, 29, 30, 31, 32, 33, 34, 35, 36, 37, 38, 39, 40, 41, 42, 43, 44, 45, 46, 47, 48, 49, 50]. Perez Sanchez et al. [33] reported studies on copper in moderate alkaline aqueous solutions containing sodium carbonate. They identified, in the region of Cu(II) species, the precipitate $CuCO_3$.-$Cu(OH)_2$ (malaquite), as long as soluble ionic Cu species were produced. The precipitation of carbonates occurred principally around pits. They state that the process becomes more noticeable at lower pH values. Milosev et al. [36] noted that an increase in the HCO_3^- concentration, electrode potential and/or passivation time promoted the formation of a stable layer consisting of a precipitated Cu(II) oxidation product covering the underlying Cu_2O layer. According to Milosev et al. [36], this second Cu(II) layer is essential for copper passivity. At $[HCO_3^-] \geq 0.05$ M, the surface film is protected against breakdown, whereas the presence of chloride ions in solution stimulates it. The authors [36] have concluded that in bicarbonate/sulfate-containing solutions the ratio $[HCO_3^-]/[SO_4^{2-}]$ is determinant for avoiding or promoting pitting. Beyond a certain potential, which increases with the solution pH, copper pitting takes place. This potential is strongly dependent on the nature and concentration of the aggressive anions [30, 31, 34, 35, 47].

In the presence of chloride the mechanism generally accepted for copper electrodissolution depends on the chloride concentration. At chloride concentrations lower than 1 M, according to Deslouis et al. [46] and Lee and Nobe [40], among others, the process is due to the following oxidation reactions:

$$Cu + Cl^- \rightarrow CuCl(s) + e^- \quad E_e = +0.137 - 0.0591\log[Cl^-] \tag{10}$$

$$CuCl + H_2O \rightarrow CuO + Cl^- + 2H^+ + 2e^- \quad E_e = +1.00 - 0.118pH + 0.059\log[Cl^-] \tag{11}$$

$$Cu + 2Cl^- \rightarrow CuCl_2^- + e^- \quad E_e = +0.208 + 0.059\log[CuCl_2^-] - 0.118\log[Cl^-] \tag{12}$$

$$CuCl_2^- + H_2O \rightarrow CuO + 2Cl^- + 2H^+ + 2e^- \quad E_e = +1.00 - 0.118pH + 0.059\log[Cl^-] \tag{13}$$

$$Cu + 2Cl^- \rightarrow CuCl_2 + 2e^- \quad E_e = +0.354 - 0.0591\log[Cl^-] \tag{14}$$

$$Cu_2O + Cl^- + 2H_2O \rightarrow Cu_2(OH)_3Cl + H^+ + 2e^- \quad E_e = +0.451 - 0.029pH - 0.029\log[Cl^-] \tag{15}$$

$$CuCl_2 \rightarrow Cu^{2+} + 2Cl^- + e^- \quad E_e = +0.618 - 0.059pH \tag{16}$$

$$2CuCl_2 + 3H_2O \rightarrow Cu_2O_3 + 4Cl^- + 6H^+ + 2e^- \quad E_e = +2.28 + 0.177pH + 0.118\log[Cl^-] \tag{17}$$

Copper oxides and copper chlorides constitute the passivating layer but complex ions may also be formed, i.e. as $CuCl_2^-$, $CuCl_3^-$, etc. These complex ions may diffuse through the solution, out of the electrode surface. Breakdown of the CuCl layer may result in pitting corrosion of copper, as reported by Chialvo et al. [47], who studied the kinetics of pitting corrosion of copper in borate buffer solutions containing sodium chloride.

According to Mankowski [35], in chloride/sulfate-containing solutions, pit morphology and the mechanism of pitting depend on the relative concentrations of both anions. For higher concentrations of Cl^- ions, chloride is responsible for the pitting. This must be the case for Cu in synthetic seawater (0.5 M NaCl + 0.03 M Na_2SO_4).

In the presence of sulfate ions, brocanthite may be formed by chemical and/or electrochemical reactions, i.e.:

$$4Cu + SO_4^{2-} + 6H_2O \rightarrow CuSO_4 \cdot 3Cu(OH)_2 + 6H^+ + 8e^-$$
$$E_e = +0.451 - 0.0444pH - 0.0074\log[SO_4^{2-}] \quad (18)$$

$$4Cu^+ + SO_4^{2-} + 6H_2O \rightarrow CuSO_4 \cdot 3Cu(OH)_2 + 6H^+ + 4e^-$$
$$E_e = +0.383 - 0.088pH - 0.0591\log[SO_4^{2-}] \quad (19)$$

$$2Cu_2O + 4H_2O + SO_4^{2-} \rightarrow CuSO_4 \cdot 3Cu(OH)_2 + 2H^+ + 4e^-$$
$$E_e = +0.433 - 0.0296pH - 0.0148\log[SO_4^{2-}] \quad (20)$$

$$4CuO + SO_4^{2-} + 2H_2O + 2H^+ \rightarrow CuSO_4 \cdot 3Cu(OH)_2 \quad (21)$$

X-ray diffraction and XPS data reported by Mankowski [35] have identified, on copper exposed in chloride aqueous solutions, pits topped by an atacamite cap and the surface with a layer of CuCl, while in solutions containing only sulfates, copper is denuded under the caps. These passivating layers present a duplex structure of copper hydroxide and brochantite, $CuSO_4.3Cu(OH)_2$. Brossard [37] reported SEM micrographs of Cu electrode surfaces after anodization at 0.00 V, exhibiting a large number of isolated spike-like crystals of different size. These crystals were identified by EDAX as CuCl.

The passivation of copper in sulfate/chloride-containing solutions is due to films composed of CuO_2, CuCl, $CuO/Cu(OH)_2$, Cu_2Cl, $Cu_2Cl.(OH)_3$ (atacamite) and/or $CuSO_4.3Cu(OH)_2$ (brochantite), depending on the polarization potentials and on the relative concentrations of Cl^- and SO_4^{2-} ions.

Bech-Nielsen et al. [50], based on Auger measurements, report for copper exposed in chloride solutions, at open circuit potential, a mixed $CuCl/Cu_2O$ layer at the earliest times followed by later growth of pure Cu_2O (thin layer). According to Sutter et al. [44], Cu_2O is the main compound on the surface layer formed on Cu in 0.5 M aerated chloride solution, under open circuit potential. Sutter et al. [44] have attributed the formation of the cuprous oxide, Cu_2O, partly by the hydrolysis of $CuCl_2^-$ within the diffusion layer.

Most of the processes involved in the electrodissolution, passivation and transpassivation of Cu in aqueous solutions, particularly in the presence of aggressive anions, lead to the formation of protons. Thus in non-buffered media, local acidification occurs.

In spite of the large amount of cyclic voltammetric studies of copper in aqueous solutions, no systematic studies exist for copper in buffered and non-buffered chloride aqueous solutions. On the other hand, the synergetic effects of Cl^- and SO_4^{2-} have been reported, but no systematic studies exists for Cu in seawater, a solution constituted by 0.5 M NaCl, 0.03 M Na_2SO_4 and minor amounts of other anions, i.e. F^- and HCO_3^-.

In real systems, i.e. seawater, dissolved oxygen is present; however, most of the studies of copper in aqueous chloride solutions reported in the literature deal only with deoxygenated solutions. Besides that, studies on the corrosion of copper in seawater are scarce.

Therefore, we have decided to start a study on the corrosion, passivation and breakdown of passivity of copper in deoxygenated and non-deoxygenated, buffered and non-buffered chloride solutions of pure chloride and of synthetic seawater.

Experimental

Copper electrodes were made from a copper rod (Goodefellows, 99.99% purity). A three-electrode two-compartment cell was used for cyclic voltammetric studies. The secondary electrode was a platinum foil and the reference electrode was a commercial saturated calomel electrode (SCE) connected to the main compartment of the cell by a Luggin capillary.

The working electrode was mechanically polished with alumina powder down to 0.05 μm, then rinsed several times with distilled water and finally dried with acetone. Before each voltammetric experiment the copper electrode was polarized for 1 min at about −1.3 V vs. SCE. Dissolved O_2 was removed by bubbling N_2 (L' Air Liquide).

Synthetic seawater solutions were prepared with pure water, from a Millipore system, and "Sea Salts Sigma Cell Culture". The composition of synthetic seawater is the following: 0.5 M NaCl + 0.03 M Na_2SO_4 + 0.002 M $NaHCO_3$ + 0.0001 M NaBr + 0.0005 M H_3BO_3. The borax buffer (pH 7.0) was prepared with boric acid (0.5 M H_3BO_3) and borax (25 mM $Na_2B_4O_7$).

Cyclic voltammetric studies were performed via a modular automated acquisition system (Autolab, Eco Chemie) composed of a potentiostat (PSAST 10), a digital/analog converter (DAC124) and an analog/digital converter (ADC 124), connected to a personal computer equipped with an appropriate program (GPES) for data acquisition.

Open circuit potential measurements were performed with copper samples immersed in a flask connected to the compartment of the reference electrode via a KNO_3 salt bridge. An HP 34 401A digital multimeter connected by an interface (RS-232) to an IBM PC model 80286 allowed automatic data acquisition over a 3-month period.

Scanning electron micrographs were obtained with a microscope from JEOL, model JSM-5200LV. Samples were treated following the procedure described in ISO/DIS 8407.

Results and discussion

Cyclic voltammetric data

Cyclic voltammograms (CVs) from copper in non-deoxygenated and deoxygenated buffered aqueous solutions of synthetic seawater are given in Fig. 1. The data show that when the anodic scan does not reach the transpassive region the shapes of the CVs do not show significant differences due to the presence of dissolved oxygen. The CV corresponding to non-deoxygenated solutions, for $E_{\lambda a} = -0.1$ V, presents a cathodic charge, $Q_c > Q_a$, while in the deoxygenated solution, $Q_a > Q_c$. This is due to the fact that in the first case the cathodic charge contains also the contribution of the reduction reaction of O_2.

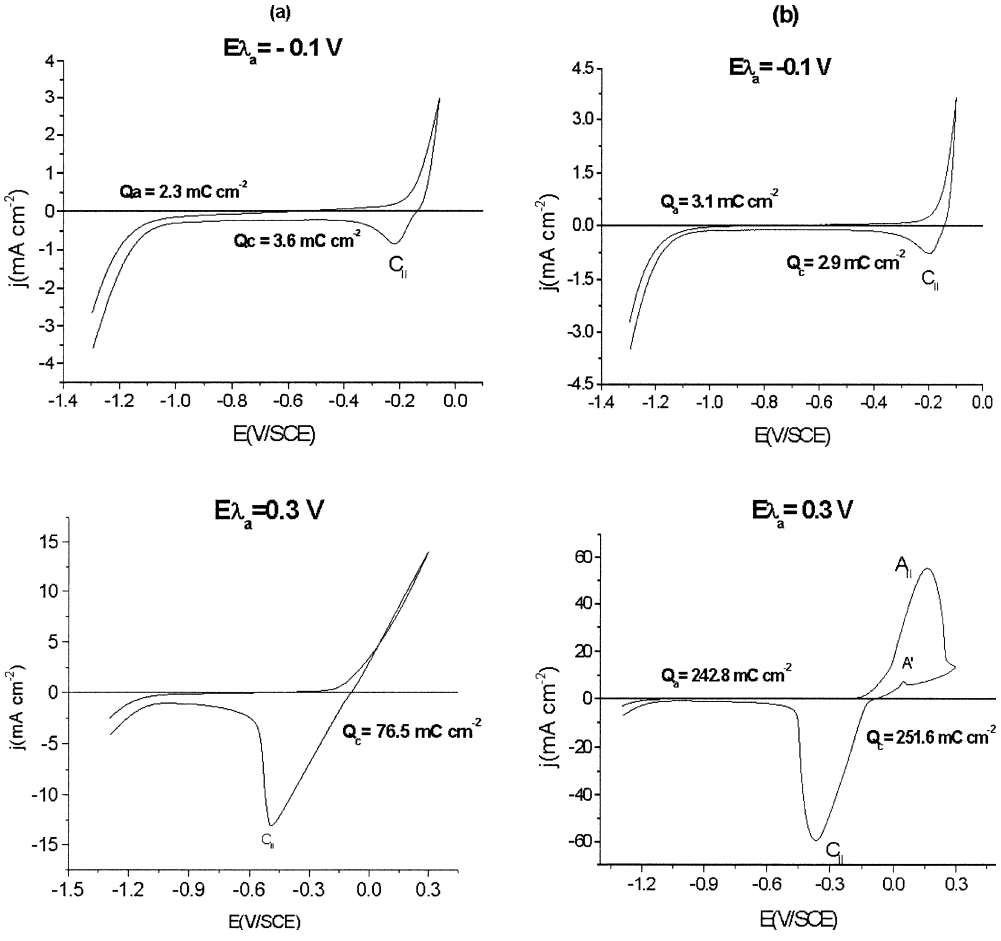

Fig. 1 Cyclic voltammograms of Cu in buffered aqueous solutions of synthetic seawater at pH 7.0 $v = 50$ mV s^{-1}: (**a**) non-deoxygenated and (**b**) deoxygenated solutions

When the anodic limit reaches the transpassive region, i.e. for $E_{\lambda a} = 0.3$ V vs. SCE, the charges and peak potentials show large differences. In non-deoxygenated solutions the crossover of the anodic currents is observed much earlier, with a value for $E_{repass} = +0.060$ V vs. SCE, while in deoxygenated solutions no crossover is observed until $E_{\lambda a} = 0.3$ V. Thus we may conclude that a more stable film is formed in deoxygenated solutions.

On the other hand, in non-deoxygenated media the CV shows an abrupt increase in current at about 0.0 V, while in deoxygenated media, under the same experimental polarization conditions, a well-defined anodic peak is recorded at +0.100 V vs. SCE. This peak may be assigned to reactions such as those given by Eqs. 4, 5, 11, 12, 14, 15 and/or 20, according to the reversible potentials in Table 1. Crousier et al. [41], Sutter et al. [44] and Chialvo et al. [47], among others, have observed a similar peak from Cu in pure chloride deoxygenated solutions, which they have attributed to the formation of $CuCl_2^-$ species by an electrochemical reaction (Eq. 12) followed by a chemical reaction, i.e.:

$$CuCl_2^- \rightarrow CuCl + Cl^- \qquad (22)$$

A small anodic peak, peak A′, is observed at +0.025 V vs. SCE, during the reverse scan. This peak is related to the presence of SO_4^{2-}, as will be demonstrated below.

Table 1 Equilibrium potentials for the redox couples of Cu in aqueous solutions of pH 7.0, [NaCl] = 0.5 M and [Na_2SO_4] = 0.03 M

Redox couple	E_e (V_{SHE})	E_e (V_{SCE})
H_2O/H_2	−0.413	−0.655
Cu/Cu_2O	+0.057	−0.185
Cu/CuO	+0.137	−0.105
$Cu/CuSO_4.3Cu(OH)_2$	+0.153	−0.091
$CuCl/Cu_2(OH)_3Cl$	+0.171	−0.071
$Cu/CuCl$	+0.178	−0.064
$CuCl/CuO$	+0.192	−0.050
$Cu/Cu(OH)_2$	+0.195	−0.047
$Cu_2O/CuSO_4.3Cu(OH)_2$	+0.204	−0.038
Cu_2O/CuO	+0.256	+0.015
$Cu_2O/Cu_2(OH)_3Cl_2$	+0.257	+0.014
$Cu/CuCl_2$	+0.371	+0.130
$CuCl_2/Cu^{2+}$	+0.599	+0.317
O_2/OH^-	+0.816	+0.574
$CuCl_2/Cu_2O_3$	+0.887	+0.645
CuO/Cu_2O_3	+1.234	+0.998

In the absence of O_2, the cathodic peak, C_{II}, appears at less negative potentials, −0.36 V against −0.51 V vs. SCE in the presence of O_2. This means that, in the ab-

sence of O_2, different basic copper chloride salts are formed that present a more positive reduction potential.

The data show clearly that the corrosion process of Cu, in deoxygenated media, presents faster kinetics and much higher oxidation charges, but pitting is displaced to more positive potentials. This may be due to the formation of thicker films that are more adherent and less porous.

In order to obtain a better understanding of the role played by the buffer, copper electrodes were polarized potentiodynamically, in boric acid/borax buffered solutions, in the absence and in the presence of the seawater salts (see data in Fig. 2). The CVs, recorded under similar experimental conditions, show large differences. Copper in boric acid/borax (pH 7.0) gives CVs with two small but well-defined cathodic peaks, located at −0.13 and −0.39 V vs. SCE. The addition of sea salts leads to CVs showing only one large anodic peak, at +0.16 V, with the corresponding cathodic peak at −0.36 V vs. SCE. Most probably this cathodic peak, at +0.36 V, can be assigned to the reduction of CuCl to Cu (Eq. 10).

In the absence of seawater, current peaks A_I and A_{II} can been assigned to the formation of Cu_2O and to a complex hydrous CuO, respectively. The negative scan shows the current peaks C_{II} and C_I, which are related to the electroreduction of CuO to Cu_2O and of Cu_2O to Cu, respectively. According to Babic et al. [16], the average composition of the outer oxide layer could be represented as $CuO_x(OH)_{2-2x}$, with x ranging between 0 and 1. The outer part of the Cu(II) oxide layer formed during increased anodic polarization and longer oxidation times is less hydrated and its reduction potential is more negative than the more hydrated Cu(II) oxide layer [16, 18].

In synthetic seawater, the presence of chloride and sulfates, in concentrations of the order of 0.5 M and 0.03 M, respectively, explains the differences in the peak potentials and charges corresponding to the cyclic voltammetric response of Cu. The anodic peak, A_{II}, recorded at +0.16 V vs. SCE, may be related with the formation of a film of complex composition, i.e. made of copper(II) oxide/copper(II) hydroxide + copper(II) chloride/copper(II) sulfates.

The anodic charges under the CVs of copper in buffered seawater for $E_{\lambda a} = 0.3$ V are quite high, in comparison to the corresponding ones without seawater (242.8 against 8.0 mC cm^{-2}, respectively).

Sea salts play a definite role in the kinetics of the corrosion process of copper in buffered aqueous solutions. Under the same experimental polarization conditions (anodic potential and oxidation time), the anodic and cathodic charges have shown an increase by a factor of about 40.

Figure 3 shows the effect of buffering the synthetic seawater. Differences related to buffering are clearly visible in the CVs recorded at the two anodic limits. For $E_{\lambda a} = -0.1$ V during the forward sweep, in the absence of buffer, one anodic peak, located at −0.19 V vs. SCE, is

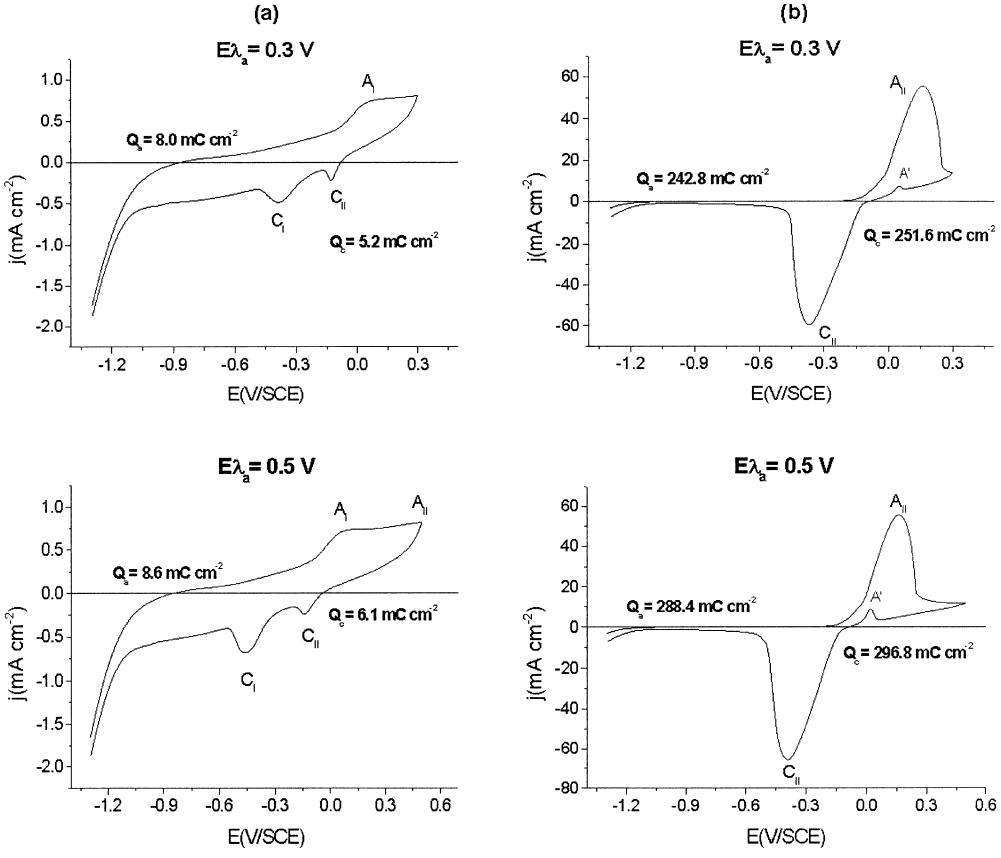

Fig. 2 Cyclic voltammograms of Cu in deoxygenated aqueous solutions of: (**a**) boric acid/borax; (**b**) boric acid/borax + synthetic seawater; $v = 50$ mV s^{-1}; pH 7.0

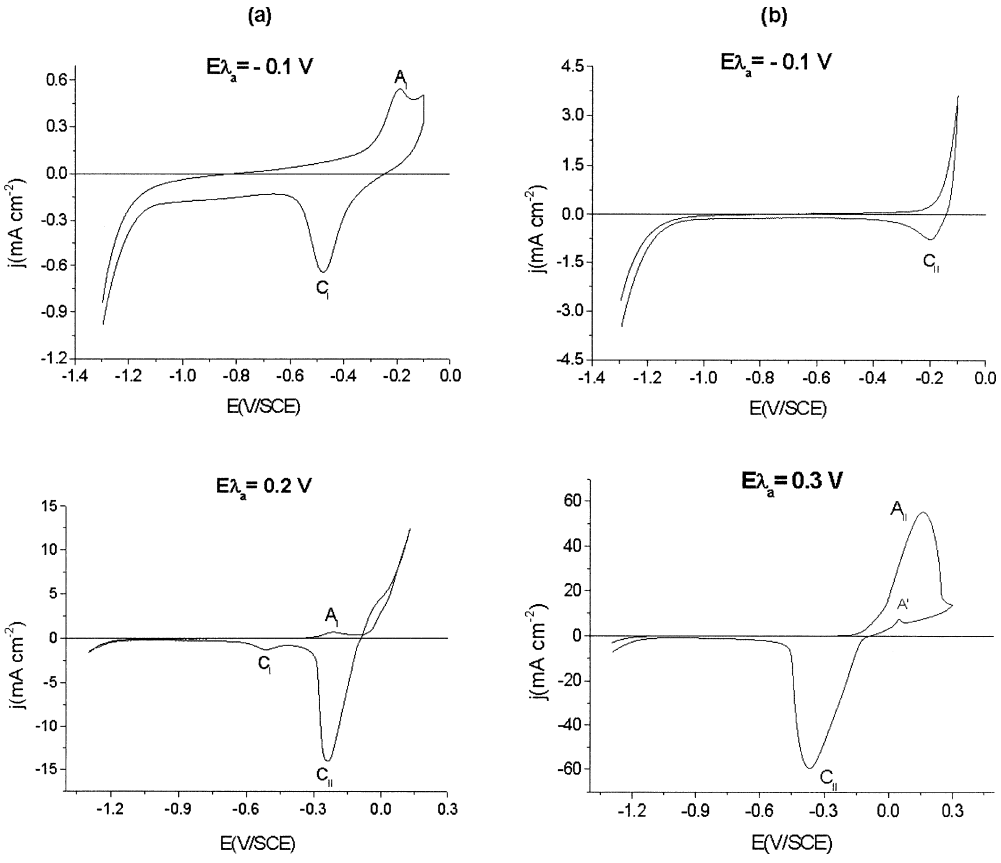

Fig. 3 Cyclic voltammograms of Cu in deoxygenated aqueous solutions of synthetic seawater: (**a**) non-buffered and (**b**) buffered solutions; $v = 50$ mV s^{-1}

observed, while in the buffered solution, no anodic peak is seen, only an increase in current starting at around −0.18 V vs. SCE. During the reverse sweep for both systems a cathodic peak, C_{II}, is observed at −0.36 and −0.180 V vs. SCE in the non-buffered and buffered solutions, respectively. This is an indication that the film growth process is favoured in the buffered media.

Anodic excursions of potential extended into the transpassive region, i.e. until +0.2 or +0.3 V, lead to CVs showing large differences related to the buffering conditions. In the non-buffered media the anodic profile of the CV shows a small anodic peak, A_I, at −0.22 V, followed by an exponential increase in current at about 0 V vs. SCE. The cathodic side of the corresponding CV shows a well-defined cathodic peak, peak C_{II}, at −0.24 V and a small peak, C_I, at −0.51 V vs. SCE. Current peak C_{II} is due to the reduction of Cu(II) oxides, and/or other complex chloride or sulfate species, to compounds involving Cu(I), whereas peak C_I can be attributed to the reduction of Cu(I) species to Cu(0).

No signs of the rupture of passivity are displayed by the CVs for Cu in buffered solutions of synthetic seawater, even when the anodic potentials reach a value of 0.3 V. Such signs are only observed when the polarization potential reaches higher values (see data of Fig. 4). According to Fig. 4 the repassivation potentials of Cu, in the non-buffered and buffered synthetic seawater, are −0.12 and +0.46 V vs. SCE, respectively. These data are in agreement with Arvia and co-workers [47], who state that buffering aqueous solutions inhibits the nucleation of pits. On the other hand, in the absence of buffer, local acidification occurs due to the protons produced by the reactions, i.e. Eqs. 1, 2, 3, 4, 6, 7, 13, 17, 18, 19 and 20 that may favour the dissolution of the passivating layers or may lead to more porous and less adherent films.

Figure 5 shows CVs from copper in buffered aqueous solutions of various concentrations of NaCl with polarizations reaching the transpassive region, i.e. for $E_{\lambda a} = 0.3$ V vs. SCE. At low concentrations (0.1 mol dm^{-3}) the cathodic profile of the CV corresponding to a reversal potential of +0.3 V shows a quite complex pattern, with three cathodic peaks at −0.18, −0.26 and −0.66 V vs. SCE, respectively, and one well-defined anodic peak, at +0.100 V vs. SCE, preceded by a small shoulder. The two first cathodic peaks may be associated with the electroreduction of solid and soluble copper(II) species, while the peak at the most negative potential is related to the reduction of Cu(I) species to Cu(0). As the concentration increases the cathodic profile tends to a simpler one showing only one cathodic peak located at −0.36 V vs. SCE.

For the purpose of comparison, cyclic voltammograms of Cu in synthetic seawater and in solutions containing chlorides and sulfates, in concentrations identical to those of seawater, i.e. 0.5 M NaCl and 0.5 M NaCl + 0.03 M Na_2SO_4, were run under similar experimental conditions. The corresponding CVs are given in Fig. 6. They do not show any significant dif-

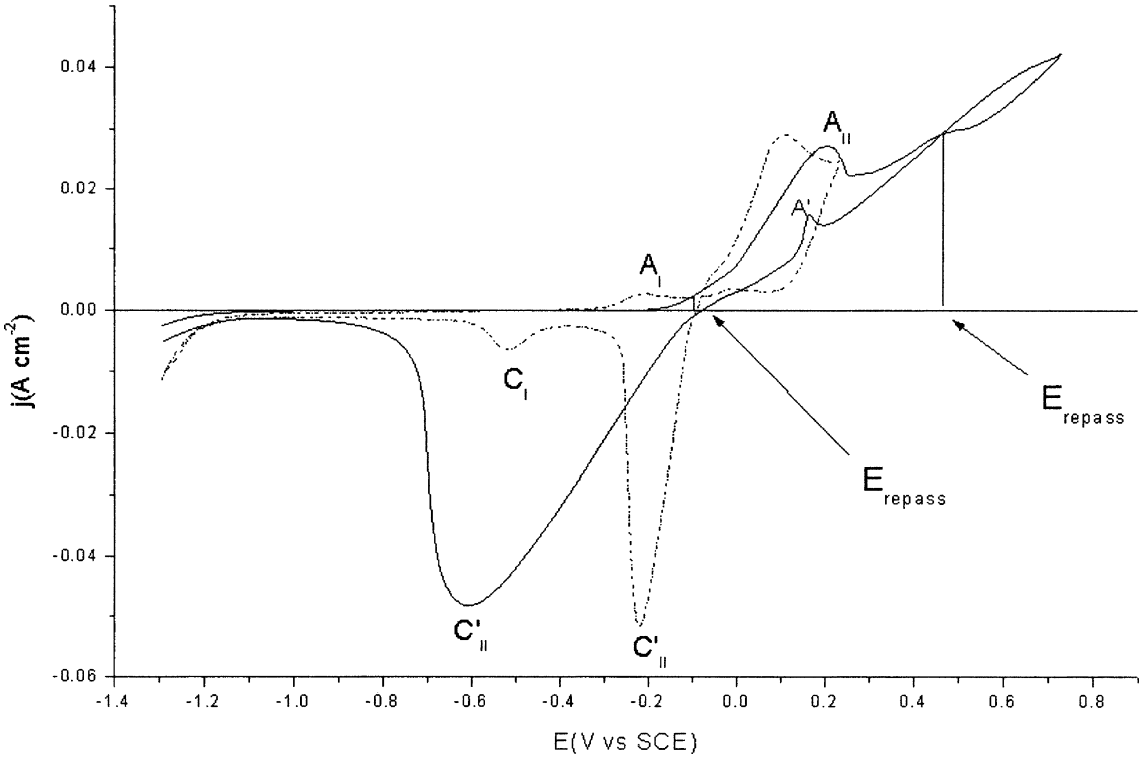

Fig. 4 Cyclic voltammograms of Cu in deoxygenated synthetic seawater with polarizations reaching the transpassive region: non-buffered (*dashed line*) and buffered (*solid line*) solutions; $v = 50$ mV s^{-1}

ferences. Only the small peak A′, at +0.025 V vs. SCE, is seen in synthetic seawater or in solutions containing SO_4^{2-}, but not in pure chloride solutions. Thus we may conclude that this peak is related to the presence of SO_4^{2-} ions.

Sweeping the potential at a low sweep rate, i.e. 1 mV s^{-1}, leads to well-defined peaks with charges much higher then those corresponding to CVs recorded at higher sweep rates, i.e. at 50 mV s^{-1} (Fig. 7). Under slow potentiodynamic polarization, films of higher thickness are produced. The ratio between the cathodic and anodic charges approaches unity. It can be concluded that almost all the anodic charge leads to deposited species that can be reduced during a slow potential sweep. Our conclusions are in agreement with data reported by Babic et al. [16].

Table 2 summarizes data from CVs recorded at slow sweep rates, i.e. 1 mV s^{-1}, for the various systems under study. From the data in Table 2 one may conclude that:

1. In buffered media, for $E_{\lambda a} = 0.0$ V vs. SCE the charges under the anodic side of the CVs, recorded at 1 mV s^{-1}, follow the order: Q_a(Cu|synthetic seawater) = 542 < Q_a(Cu|0.5 M NaCl + 0.03 M Na_2SO_4) = 565 < Q_a(Cu|0.5 M NaCl) = 628 mC cm^{-2}.
2. On the other hand, the corresponding cathodic charges follow the order: Q_c(Cu|0.5 M NaCl + 0.03 M Na_2SO_4) = 385 < Q_c(Cu|0.5 M NaCl) = 450 < Q_c(Cu|synthetic seawater) = 475 mC cm^{-2}.

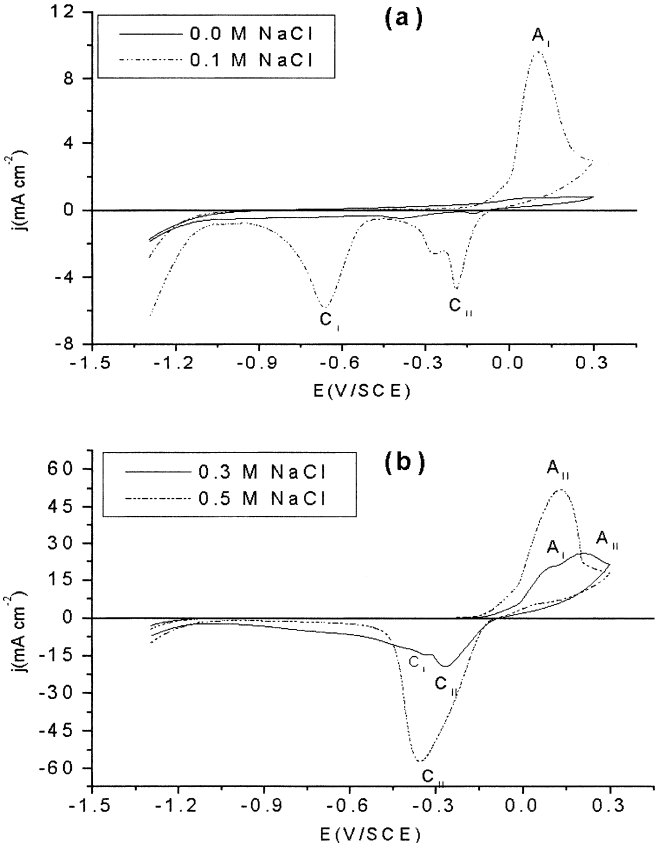

Fig. 5 Cyclic voltammograms of Cu in deoxygenated aqueous solutions of x M NaCl + boric acid/borax; $v = 50$ mV s^{-1}; pH 7.0

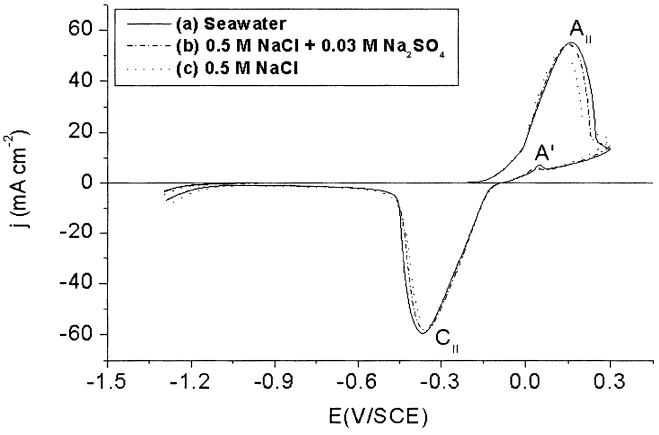

Fig. 6 Cyclic voltammograms of Cu in deoxygenated buffered aqueous solutions of synthetic seawater (*solid line*), 0.5 M NaCl + 0.03 M Na_2SO_4 (*dashed line*) and 0.5 M NaCl (*dotted line*); pH 7.0; $v = 50$ mV s^{-1}; $E_{\lambda a} = 0.3$ V vs. SCE

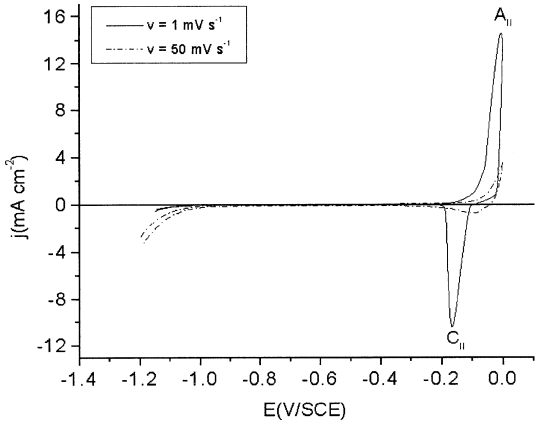

Fig. 7 Cyclic voltammograms of Cu in deoxygenated buffered aqueous solutions of synthetic seawater at two sweep rates: $v = 50$ mV s^{-1} (*dashed line*) and $v = 1$ mV s^{-1} (*solid line*); pH 7.0; $E_{\lambda a} = 0.0$ V vs. SCE

The corrosion potentials, E'_{corr}, follow an order similar to that of the cathodic charges, i.e.: E_{corr}(Cu|0.5 M NaCl) = −0.570 < E_{corr}(Cu|0.5 M NaCl + 0.03 M Na_2SO_4) = −0.54 < E_{corr}(Cu|synthetic seawater) = −0.400 V vs. SCE.

Buffered synthetic seawater is less aggressive for Cu than the corresponding solutions containing only chlorides or chloride and sulfates in the same amount as in seawater. Most probably, the other anions present in seawater, such as bromide, may contribute to reduce the aggressiveness of chlorides and sulfates. On the other hand, the major corrosive effects of seawater are necessarily due to the presence of chlorides, since the addition of sulfates leads only to very small differences; however, it should be mentioned that the concentrations in Na_2SO_4 are quite low in comparison with those of NaCl.

For Cu in deoxygenated, buffered pure chloride solutions the anodic and cathodic charges increase almost linearly with the concentration of Cl^- (see plots of Fig. 8). In fact, chloride contributes to increase the amount of soluble species, most probably through the formation of copper chloride complexes. As mentioned in the relevant literature, the adsorption of Cl^- is enhanced by increasing the anodic potential and/or by increasing the chloride concentration. The adsorbed Cl^- ions participate directly in the elementary steps of ionization through the pores of the oxide and/or copper chloride layer [47, 48].

Weight loss measurements

Weight loss studies, performed under identical conditions to those used for the open circuit potential measurements, of Cu samples immersed in aqueous solutions of synthetic seawater and 0.5 M in NaCl, have lead to the results presented in the graphic of Fig. 9. The data show a maximum in the corrosion rates after about 1 month of exposure followed by a decrease to a minimum of 26 and 38 μg cm^{-2} d^{-1} after about 3 months. Then, during the next 3 months, a continuous increase in V_{corr}, at rates of 0.49 and 0.38 μg cm^{-2} d^{-1}, is observed for Cu in 0.5 M NaCl and in synthetic seawater, respectively. These data correlate well with our conclusions from the open circuit potential measurements (below).

Open circuit potential measurements

Figure 10 gives the open circuit potential curves of copper in non-deoxygenated buffered and non-buffered synthetic seawater, over a three-month period. The buffered solution gives oscillations in the open circuit potential, of high amplitude and quite frequent, only after about 40 days of exposure, while Cu in the non-buffered solution gives oscillations of quite high amplitude from the beginning of the exposure.

Table 2 Charges and peak potentials from CVs of Cu, recorded at 1 mV s^{-1}; $E_{\lambda a} = 0.0$ V vs. SCE

System	Q_a	Q_c	Q_a/Q_c	E'_{corr}	$E_p{}^{A}{}_{II}$	$E_p{}^{C}{}_{I}$	$E_p{}^{C'}{}_{II}$
	(mC cm^{-2})			(V vs. SCE)			
Cu|0.5 M NaCl, pH 7.0	628	450	1.4	−0.57	−0.012	−0.20	−0.16
Cu|0.5 M NaCl, without buffer	611	450	1.4	−0.55	−0.012	–	−0.16
Cu|synthetic seawater, pH 7.0	542	475	1.4	−0.40	−0.007	–	−0.17
Cu|synthetic seawater, without buffer	716	375	1.9	−0.45	−0.023	–	−0.16
Cu|0.5 M NaCl + 0.03 M Na_2SO_4, pH 7.0	565	385	1.5	−0.54	−0.013	–	−0.15

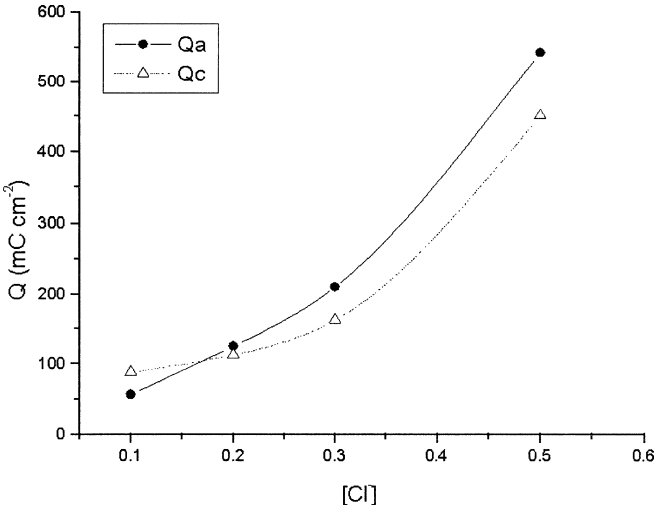

Fig. 8 Plots of the anodic and cathodic charges, from CVs of Cu in buffered NaCl aqueous solutions of various concentrations; $E_{\lambda a} = 0.0$ V vs. SCE; $v = 1$ mV s^{-1}; pH 7.0

Open circuit potential measurements lead us to conclude that in buffered media more stable passivating layers are formed. Passivation of copper occurs and is maintained during longer periods in buffered solutions of synthetic seawater. According to Arvia and colleagues [47], buffering inhibits the nucleation of pits.

Bech-Nielsen et al. [50], based on Auger measurements, report for copper exposed in chloride solutions, at open circuit potential, a mixed $CuCl/Cu_2O$ layer at the earliest times followed by later growth of pure Cu_2O (thin layer).

Millet et al. [43] have found differences in the electrochemical reduction curves of oxide layers grown on Cu in aerated 0.1 M sodium acetate/0.5 M NaCl solution, at open circuit potential, as the immersion time advances. From XPS measurements they have concluded that in the oxide layers, in some cases, an evolution of the oxidation state of copper from +2 to +1 occurs.

SEM micrographs

Micrographs from copper samples exposed over a three-month period, in non-deoxygenated buffered synthetic seawater and in 0.5 M NaCl aqueous solutions, are given in Figs. 11 and 12. Deep pits with a round shape covered by copper salts have been observed. The density of the pits is higher on samples immersed in the 0.5 M NaCl aqueous solution in comparison with those immersed in synthetic seawater.

Our studies are planned to continue, particularly focused on the analysis of SEM images (pitting density determinations and identification of the corrosion products around the pits and on the surface).

Conclusions

Cyclic voltammetric data

Deoxygenation leads to faster kinetics and to much higher oxidation charges; however, pitting is displaced to much more positive potentials.

Sea salts play a definite role in the kinetics of the corrosion process of copper in buffered aqueous solutions. Under the same experimental polarization conditions, the anodic and cathodic charges associated with the corresponding CVs, recorded at 50 mV s^{-1}, have shown an increase by a factor between 30 and 50, depending on the experimental conditions.

Buffering influences strongly the voltammetric response of Cu in synthetic seawater and in chloride solutions: the shape, number and size of voltammetric peaks is strongly influenced. In buffered media, CVs corresponding to $E_{\lambda a} = 0.2$–0.3 V vs. SCE, recorded at 50 mV s^{-1}, present anodic charges about 10 times higher, and pitting takes place at much higher anodic potentials. Repassivation potentials are displaced, in the positive direction, by about 400 mV.

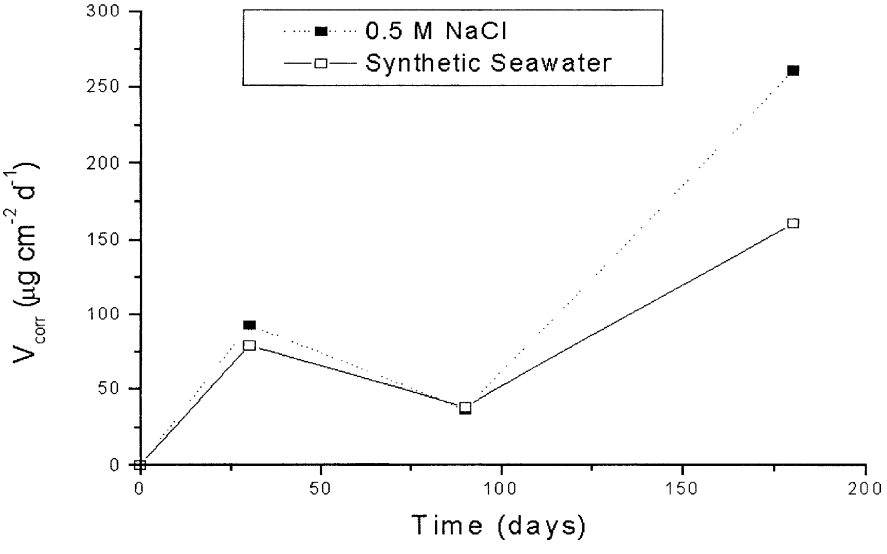

Fig. 9 Plots of V_{corr} as a function of immersion time for Cu in synthetic seawater and in 0.5 M NaCl buffered aqueous solutions

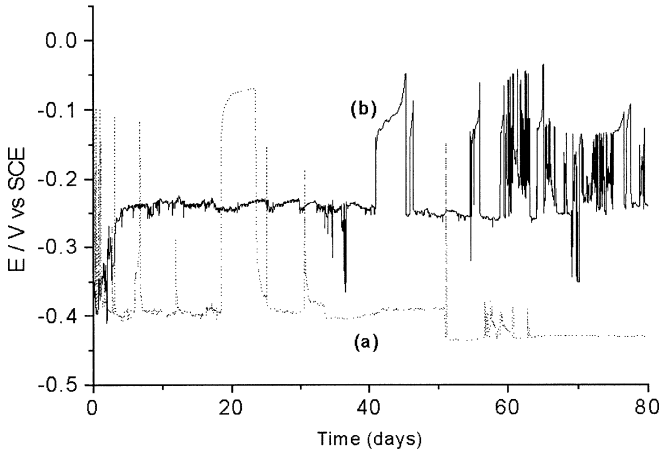

Fig. 10 Open circuit potential curves of Cu in non-deoxygenated aqueous solutions of synthetic seawater: (**a**) non-buffered and (**b**) buffered

CVs of Cu polarized between −1.30 and +0.0 V vs. SCE in deoxygenated solutions containing only chloride, recorded at 1 mV s^{-1}, show anodic and cathodic charges increasing with the concentration of Cl^-. The difference between anodic and cathodic charges increases as the concentration of chloride increases. In fact it is reported in the literature that chloride contributes to increase the amount of soluble species, most probably through the formation of copper chloride complexes.

The peak current densities of the anodic the cathodic peaks were shown to increase linearly with the chloride concentration.

CVs show clearly that sweeping the potential, at low sweep rates, leads to a well-defined pair of peaks, with charges much higher then those corresponding to CVs recorded at higher sweep rates, i.e. at 50 mV s^{-1}. Under slow potentiodynamic polarization, films of higher thickness are certainly produced. At low sweep rates, the ratio between the cathodic and anodic charges tends to unity, indicating that almost all the anodic charge leads to deposited species that can be reduced during a slow potential sweep.

The open circuit potential transients of copper in non-deoxygenated, non-buffered synthetic seawater indicate pitting from the beginning of the exposure, in agreement with voltammetric data, while for copper in buffered solutions, oscillations, indicative of pitting, appear only after a quite long exposure period, i.e. after 40 days.

Data from weight loss studies are in quite good agreement with the conclusions from open circuit potential measurements: copper starts to corrode during the initial period of immersion, leading to the formation of a passivating film. Then, after a three-month period, V_{corr} starts to increase, at quite a high rate, reaching higher values in 0.5 M NaCl solutions. Then breakdown of passivity takes place.

SEM micrographs of the copper samples with 1, 3, 6 and 9 months of immersion for both solutions show

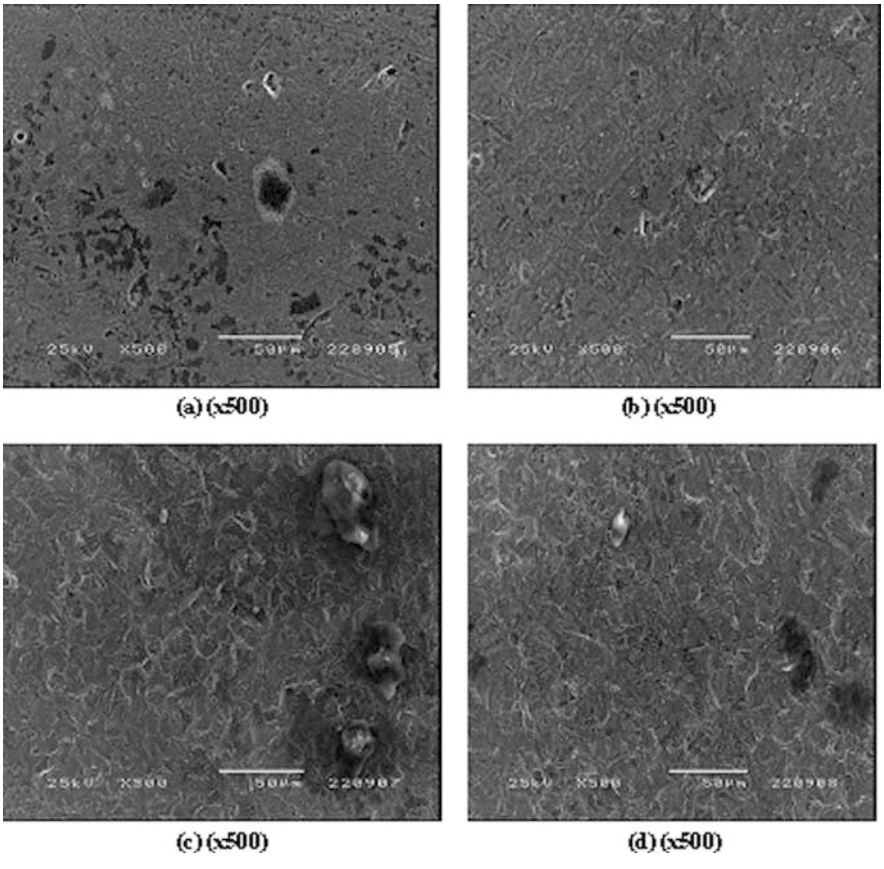

Fig. 11 SEM micrographs of copper samples after (**a**) 1 month, (**b**) 3 months, (**c**) 6 months and (**d**) 9 months of exposure in buffered synthetic seawater

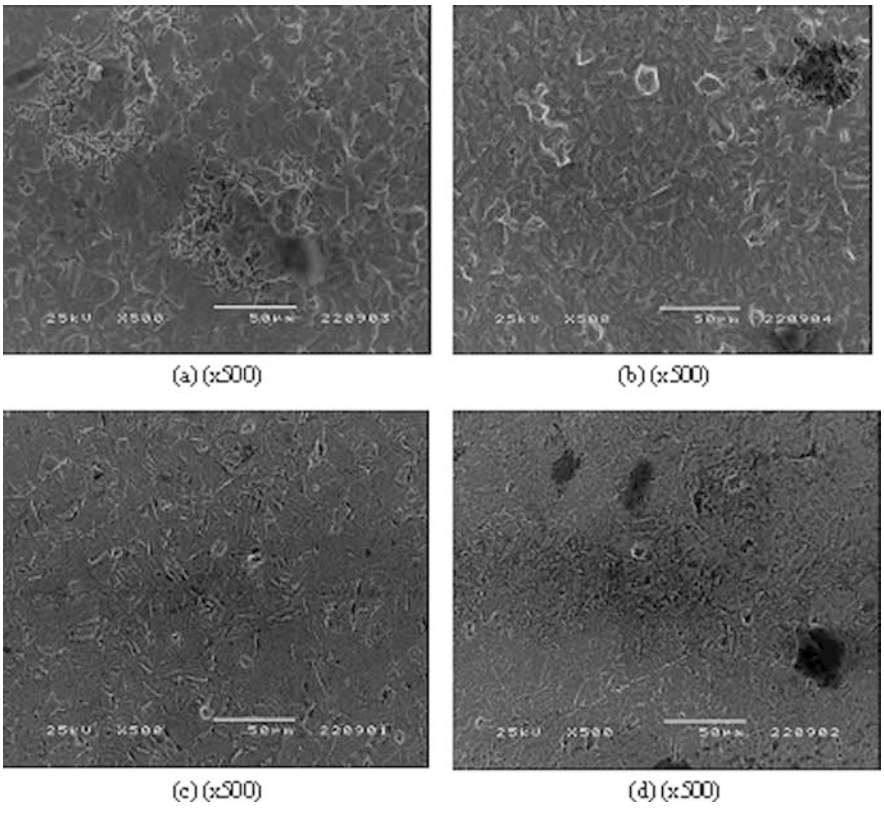

Fig. 12 SEM micrographs of copper samples after: (**a**) 1 month, (**b**) 3 months, (**c**) 6 months and (**d**) 9 months of exposure in buffered 0.5 M NaCl aqueous solution

round pits covered by copper salts. A higher density of pits is observed on samples exposed in chloride solutions (0.5 M NaCl), in comparison with those exposed in synthetic seawater.

All the studies have confirmed that synthetic seawater is somewhat less aggressive than pure chloride solutions of identical concentrations of NaCl.

Further studies for the characterization of the corrosion products on copper samples immersed in buffered and non-buffered synthetic seawater, as well as a more detailed analysis of the corroded surfaces, are in progress.

Acknowledgements The authors would like to thank Fundação para a Ciência e Tecnologia (FCT) for providing financial support to Centro de Electroquímica e Cinética da Universidade de Lisboa-CECUL – Research Unit POCTI/301/2003 (vertente FEDER). J. Ferreira thanks the FCT for a grant, in the framework of project POCTI/CTM/39846/2001.

References

1. Shams El Din AM, Abd El Wahab FM (1964) Electrochim Acta 9:113
2. Miller B (1969) J Electrochem Soc 116:1675
3. Hampson NA, Lee JB, Macdonald KI (1971) J Electroanal Chem 32:165
4. Ambrose J, Barradas RG, Shoesmith DW (1973) J Electroanal Chem 47:47
5. Macdonald DD, Owen D (1973) J Electrochem Soc 120:317
6. Macdonald DD (1974) J Electrochem Soc 121:651
7. Castro Luna AM, Marciano SL, Arvia AJ (1978) J Appl Electrochem 8:12
8. Strehblow HH, Titze B (1980) Electrochim Acta 25:839
9. Abd El Haleem SS, Ateya BG (1981) J Electroanal Chem 117:309
10. Abrantes LM, Castillo ML, Norman C, Peter LM (1984) J Electroanal Chem163:209
11. Martins ME, Arvia AJ (1984) J Electroanal Chem 136:XXX
12. Gennero de Chialvo MR, Marchiano SL, Arvia AJ (1984) J Appl Electrochem 14:165
13. Deutscher RL, Woods R (1986) J Appl Electrochem 16:413
14. Hong Pyun C, Park S (1986) J Electrochem Soc 13:2024
15. Lohrengel MM, Schultze JW, Speckmann HD, Strebhlow H-H (1987) Electrochim Acta 32:733
16. Babíc R, Metikos-Hukovíc M, Jukić A (2001) J Electrochem Soc 148:B146
17. Strehblow HH, Maurice V, Marcus P (2001) Electrochim Acta 46:3755
18. Muylder JV (1981) In: Bockris JO'M, Conway BE, Yeager E, White RE (eds) Comprehensive treatise of electrochemistry, vol 4. Plenum Press, New York, p XXX
19. Pourbaix M (1966) Atlas of electrochemical equilibria in aqueous solutions. Pergamon Press, New York
20. Al-Kharafi FM, El-Tanatanwy YA (1982) Corros Sci 1:22
21. Edwards M, Rehring J, Meyer T (1994) Corros Sci 50:366
22. Tantanwy YA, Al-Kharafi FM, Katrib A (1981) J Electroanal Chem 125:321
23. Laz MM, Souto RM, Gonzalez S, Salvarezza RC, Arvia AJ (1992) Electrochim Acta 37:655
24. Drogowsa M, Brossard L, Ménard H (1992) J Electrochem Soc 139:2787
25. Bustorff A, Muylder JV (1964) Electrochim Acta 9:60
26. Altukhov VK, Marshakov IK, Voronstov ES, Klepinina TN (1976) Elektrokhimiya 12:88
27. Correia de Sá AI (1992) MSc Thesis, Lisbon
28. Fonseca ITE, Marin ACS, Correia de Sá AI (1992) Electrochim Acta 37:2541

29. Jardy A, Lasalle-Molin AL, Keddam M, Takenouti H (1992) Electrochim Acta 37:2195
30. Souto RM, Gonzalez S, Salvarezza RC, Arvia AJ (1994) Electrochim Acta 39:XXXX
31. Fonseca ITE, Correia de Sà AI (1995) Mater Sci Forum 511:192
32. Drogowska M, Brossard L, Menard H (1992) J Electrochem Soc 139:39
33. Perez Sanchez M, Barrera M, Gonzalez S, Souto RM (1990) Electrochim Acta 35:1337
34. Duthil J, Mankowski G, Giusti A (1996) Corros Sci 38:1839
35. Mankowski G (1997) Corros Sci 27:39
36. Milosev I, Metikos M, Hukovic M, Drogowska M, Menard H, Brossard L (1992) J Electrochem Soc 139:2409
37. Brossard RL (1983) J Electrochem Soc 130:1109
38. Bjorndall WD, Nobe K (1984) Corrosion 40:82
39. Dhar HP, White RH, Burnell G, Darby R (1985) Corrosion 41:317
40. Lee HP, Nobe K (1986) J Electrochem Soc 133:2035
41. Crousier J, Pardessus L, Crousier JP (1988) Electrochim Acta 33:1039
42. Mansfeld F, Little B (1992) Electrochim Acta 37:2291
43. Millet B, Fiaud C, Sutter EMM (1995) Corros Sci 378:1903
44. Sutter EM, Millet MB, Fiaud C, Lincot D (1995) J Electroanal Chem 386:101
45. Modestov AD, Zhou GD, Ge H-H, Loo BH (1995) J Electrochem Soc 380:63
46. Deslouis C, Tribollet B, Mengoli G, Musiani MM (1988) J Appl Electrochem 18:374
47. Chialvo MR, Salvarezza RC, Vasquez Moll V, Arvia AJ (1985) Electrochim Acta 30:1501
48. Elsner CI, Salvarezza RC, Arvia AJ (1988) Electrochim Acta 33:1735
49. Awad SA, Kamel KM, Abd El-Hadi Z, Bayumi HA (1986) J Electroanal Chem199:341
50. Bech-Nielsen G, Jaskula M, Chorkendorff I, Larsen J (2002) Electrochim Acta 47:42